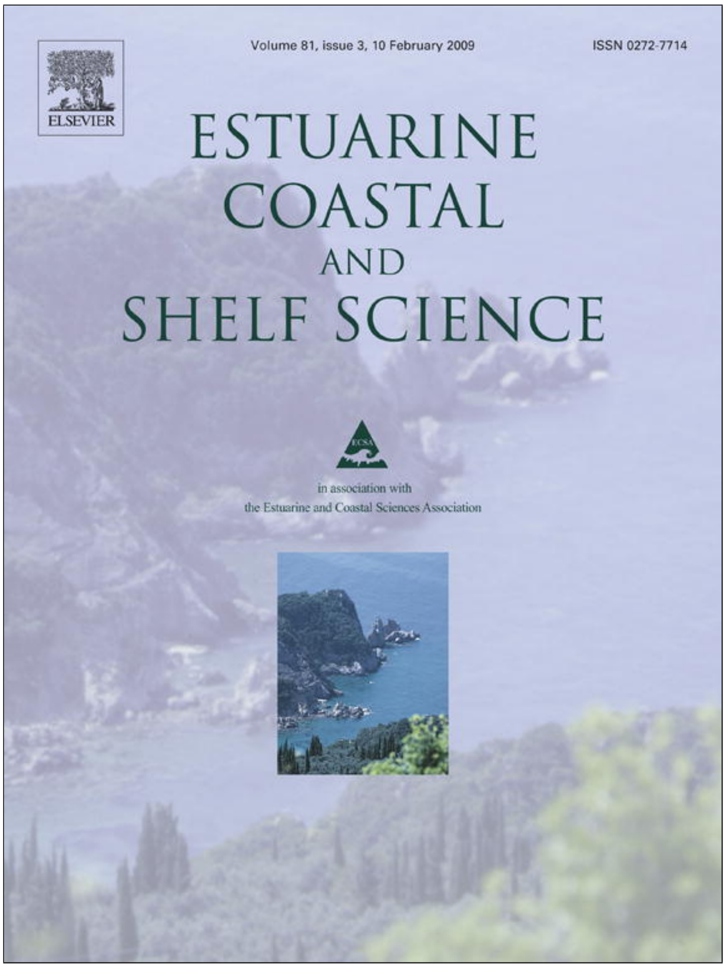

Estuarine, Coastal and Shelf Science 81 (2009) 321–332

Contents lists available at ScienceDirect

Estuarine, Coastal and Shelf Science

journal homepage: www.elsevier.com/locate/ecss

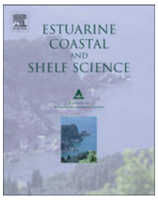

Dynamics of the turbidity maximum zone in a macrotidal estuary (the Gironde, France): Observations from field and MODIS satellite data

David Doxaran [a,*], Jean-Marie Froidefond [b], Patrice Castaing [b], Marcel Babin [a]

[a] *Laboratoire d'Océanographie de Villefranche, Centre National de la Recherche Scientifique, Université Pierre et Marie Curie, Villefranche-sur-Mer Cedex, France*
[b] *UMR-EPOC 5805, Centre National de la Recherche Scientifique, Université Bordeaux 1, Talence Cedex, France*

ARTICLE INFO

Article history:
Received 4 July 2008
Accepted 13 November 2008
Available online 27 November 2008

Keywords:
estuarine dynamics
turbidity maximum
satellite sensing
macrotidal environment
ocean color
MODIS
Gironde estuary

ABSTRACT

Over a 1-year period, field and satellite measurements of surface water turbidity were combined in order to study the dynamics of the turbidity maximum zone (TM) in a macrotidal estuary (the Gironde, France). Four fixed platforms equipped with turbidity sensors calibrated to give the suspended particulate matter (SPM) concentration provided continuous information in the upper estuary. Full resolution data recorded by the moderate resolution imaging spectroradiometer (MODIS) sensors onboard the Terra and Aqua satellite platforms provided information in the central and lower estuary twice a day (depending on cloud cover). Field data were used to validate a recently developed SPM quantification algorithm applied to the MODIS 'surface reflectance' product. The algorithm is based on a relationship between the SPM concentration and a reflectance ratio of MODIS bands 2 (near-infrared) and 1 (red). Based on 62 and 75 match-ups identified in 2005 with MODIS Terra and Aqua data, the relative uncertainty of the algorithm applied to these sensors was found to be 22 and 18%, respectively.

Field measurements showed the tidal variations of turbidity in the upper estuary, while monthly-averaged MODIS satellite data complemented by field data allowed observing the monthly movements of the TM in the whole estuary. The trapping of fine sediments occurred in the upper estuary during the period of low river flow. This resulted in the formation of a highly concentrated TM during a 4-month period. With increasing river flow, the TM moved rapidly to the central estuary. A part of the TM detached, moved progressively in the lower estuary and was finally either massively exported to the ocean during peak floods or temporary trapped (settled) on intertidal mudflats. The massive export to the ocean was apparently the result of combined favorable environmental conditions: presence of fluid mud near the mouth, high river flow, high tides and limited wind speeds. The mean SPM concentration within surface waters of the whole estuary showed strong seasonal variations but remained almost unchanged on a 1-year-basis. These observations suggest that the masses of suspended sediments exported toward the ocean and supplied by the rivers were almost equivalent during the year investigated (2005). Results show the usefulness of information extracted from combined field and current ocean color satellite data in order to monitor the transport of suspended particles in coastal and estuarine waters.

1. Introduction

The seaward export of suspended solids from rivers directly affects phytoplankton productivity, nutrient dynamics and the transport of pollutants in the coastal ocean. It is also one important component in the global carbon cycle (Schlunz and Schneider, 2000). Indeed, on a global scale, it is estimated that half the terrestrial organic carbon exported by rivers is finally buried in marine sediments, which is quantitatively equivalent to the burial of organic carbon produced in the ocean (Hedges et al., 1997; Schlunz and Schneider, 2000).

At the interface between terrestrial and ocean environments, the transport of suspended solids becomes complex and hardly predictable in estuaries where the influence of the tide leads to an increased residence time of freshwater and fine sediments (clays, silts) in a turbidity maximum zone (TM) (Dyer, 1986). As a result, the fluxes of riverine suspended solids and particulate organic carbon exported to the ocean are currently poorly documented, due to a lack of appropriate measurements that take into account the seasonal cycles of river discharges (Fettweis et al., 1998). When available, field measurements are expensive and are either specific to a time period or a geographical location (i.e. not representative of the riverine or estuarine section); they are recorded several

---

* Corresponding author.
E-mail addresses: doxaran@obs-vlfr.fr (D. Doxaran), jm.froidefond@epoc.u-bordeaux1.fr (J.-M. Froidefond).

0272-7714/$ – see front matter © 2008 Elsevier Ltd. All rights reserved.
doi:10.1016/j.ecss.2008.11.013

(sometimes hundreds of) kilometers upstream from the river mouth and do not take into account the trapping of sediments in estuaries (Ludwig et al., 1996; Schlunz and Schneider, 2000).

An operational monitoring of the TM is therefore necessary in estuarine environments. This monitoring requires regular and relevant observations which cannot be obtained from field measurements. Satellite remote sensing may represent a solution in this domain (Doxaran et al., 2002, 2006), notably with the new generation of ocean color satellite sensors (Miller and McKee, 2004) which have a spatial resolution and acquisition frequency rather well adapted to the dynamics of coastal environments. Relevant information may be obtained when combining field and satellite observations.

The objectives of this study are to describe the seasonal dynamics of the TM in a macrotidal estuary, using a new methodology which combines field and remote sensing observations. Specific aims are: (1) to determine the conditions required for export of the TM towards the ocean; and (2) to estimate the mass of sediments involved in this seaward export. The information on TM dynamics that can be obtained from a limited number of field platforms equipped with sensors is first examined. It is complemented by the information obtained from MODIS Aqua and Terra satellite data converted into surface SPM concentrations when applying a regional SPM algorithm validated using measurements on field platforms. The combined field and satellite observations are finally used to describe and better understand the tidal and seasonal dynamics of the TM.

The study area is the Gironde estuary (south-west France; Fig. 1), which is one of the largest estuaries in Europe. It is representative of macrotidal environments with a well-developed TM (Castaing and Allen, 1981). It is equipped with four autonomous fixed platforms designed for water quality monitoring. Moreover, an algorithm has recently been developed for this area to quantify SPM within surface waters from ocean color satellite data (Doxaran et al., 2002, 2003). This algorithm has been applied to a set of high spatial resolution ocean color satellite data and it was shown that such remote sensing techniques can be used to identify and locate detailed turbidity features in the estuary (Doxaran et al., 2006). The objective in this study is to go further and develop an operational tool to monitor the transport of suspended sediments in the estuary that combines daily satellite observations with autonomous field measurements.

2. Materials and methods

2.1. Field data

The Gironde estuary has been equipped with four Marel platforms since February 2004. These platforms, developed by the French Institute of Research and Exploitation of the Sea (IFREMER), are designed for monitoring water quality in riverine, estuarine and coastal environments. Measurements of temperature, salinity, dissolved oxygen and turbidity are recorded every 10 min, 1 m below the water surface, using Endress+Hauser sensors.

The four platforms are located (Fig. 1): (1) in the Dordogne River, 35 km upstream from the confluence of the Garonne and Dordogne; (2) in the Garonne River at Portets and Bordeaux, respectively 25 and 45 km upstream from the confluence zone; and (3) in the central part of the estuary, 2 km downstream from Pauillac, at kilometer point (KP) 43 (Bordeaux is the reference KP 0, and increasing KP is located downstream from Bordeaux). The location of these platforms was chosen with the aim of studying the suspected upstream displacement of the TM during the past 10 years. In order to facilitate their maintenance, they are fixed on pontoons floating approximately 10 m from the shore. Sensors are regularly calibrated. Based on calibrations performed in 2005 and 2006, the following linear relationship has been established between turbidity measurements (nephelometric turbidity units, NTU) recorded by the Endress+Hauser sensor and SPM concentration (g m^{-}3):

$$\mathrm{SPM} = 0.9946 \times \mathrm{NTU}, \quad R^2 = 0.97, \quad n = 65 \qquad (1)$$

This relationship is specific to the turbidity sensor used, but is similar to the one established by Doxaran (2002) who used an optical backscatter point sensor (OBS, D&A Instrument Company). This suggests that the SPM grain size distribution and composition in the estuary did not change significantly in optical terms over the years.

One year's worth (01/01/2005–31/12/2005) of turbidity and salinity data recorded on the four Marel platforms was considered in our analysis. The year 2005, the first year of continuous measurements carried out by the four stations, was selected despite a gap of 2 months during which no data was recorded on the Bordeaux Marel platform (01/01/2005–28/02/2005). The freshwater discharges of the Garonne and Dordogne rivers were measured daily upstream the limit of the tidal influence, respectively in La Réole (60 km upstream of Bordeaux) and Pessac-sur-Dordogne (40 km upstream of Libourne) (Fig. 1). The annual average Gironde (Garonne + Dordogne) discharge in 2005 was 562 m^3 s^{-}1 (data provided by the Port Autonome de Bordeaux). Since the annual freshwater discharge varied between 512 and 1305 m^3 s^{-}1 from 1959 to 2005 (with a mean value of 944 m^3 s^{-}1), this makes 2005 one of the driest years since 1959.

2.2. Satellite data

Two MODIS sensors are currently operational aboard the Terra and Aqua satellites. Two of their spectral channels are available at full spatial resolution (250 m): one in the visible spectral domain (B1: 620–670 nm) and one in the near-infrared (B2: 841–876 nm). This conveniently corresponds to the wavelengths needed to apply the SPM quantification algorithm developed by Doxaran et al. (2002, 2003). Two images per day (one from each MODIS sensor) are recorded over the Gironde estuary between 10:00 and 14:00 UT.

The algorithm developed by Doxaran et al. (2002, 2003) to quantify SPM concentrations in the Gironde estuary is based on a relationship between the SPM concentration and a spectral ratio of water reflectance around 850 nm to reflectance at 550 or 650 nm. This relationship was obtained from 204 simultaneous field hyperspectral (350–950 nm) reflectance spectra and concurrent SPM concentration measurements carried out between 1996 and 2006. It can be adapted to any satellite sensor spectral bands and applied to satellite data corrected for atmospheric corrections.

This algorithm has been previously applied to a limited number of SPOT-HRV (High Resolution Visible) and Landsat-ETM+ (Enhanced Thematic Mapper Plus) satellite images of the Gironde estuary (Doxaran et al., 2002, 2006). On clear days, the atmospheric effects on these satellite data were observed to be limited over the highly reflective estuarine waters. As a result, realistic SPM concentrations were retrieved despite imperfect atmospheric corrections (Doxaran et al., 2006). The high spatial resolutions of SPOT-HRV and Landsat-ETM+ sensors (20 and 30 m, respectively) proved to be useful in detecting detailed turbidity features in the estuary. However, no field measurement was carried out concurrently with the acquisition of these satellite data, so the SPM algorithm could not be validated. The first aim in this study was therefore to multiply match-ups between MODIS measurements and field data recorded on the Marel platforms, in order to assess the validity and accuracy of the algorithm. Taking into account the relative spectral responses of MODIS satellite sensors (ftp://

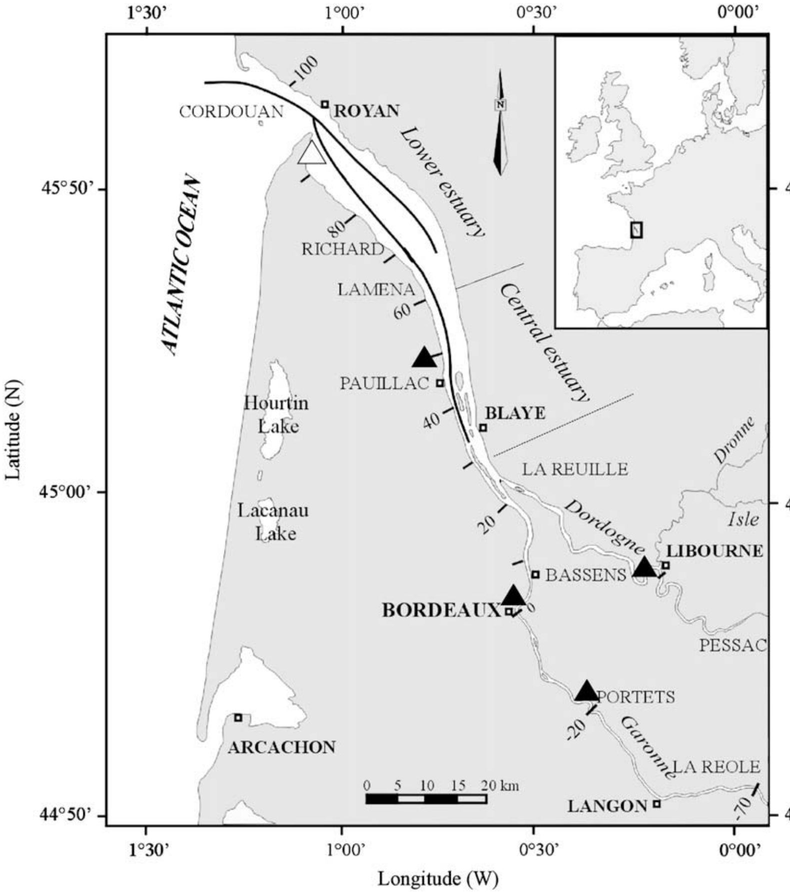

Fig. 1. Map of the Gironde estuary (South-West of France). Black lines represent the main navigation channels. Black triangles locate the four fixed Marel platforms. The white triangle locates the fifth Marel platform to be installed in 2010. Bordeaux is the reference kilometre point (KP 0), and increasing KP is located downstream Bordeaux.

ftp.mcst.ssai.biz/pub/permanent/MCST/PFM_L1B_LUT_4-30-99/ for MODIS Terra and ftp://ftp.mcst.ssai.biz/pub/permanent/MCST/FM1_RSR_LUT_07-10-01/ for MODIS Aqua), the optical database developed from field measurements was used to establish the relationship between the SPM concentration in the Gironde estuary and the MODIS B2 to B1 water reflectance ratio ($\Re_{21} = R(\mathrm{B2})/R(\mathrm{B1})$):

$$\mathrm{SPM} = 12.996 \times \exp\left(\frac{\Re_{21}}{0.189}\right), \quad R^2 = 0.89, \quad n = 204 \tag{2}$$

To map concentrations of total suspended matter in coastal waters influenced by the Mississippi River plume using 250 m MODIS Terra data, Miller and McKee (2004) used the MOD02QKM product, i.e. calibrated radiances recorded at the top of the atmosphere. The processing of such data requires at least three successive steps: (1) geolocation using fields provided at 1 km, (2) atmospheric correction; and (3) conversion into percent surface reflectance: π (in sr) × water leaving radiance (in $\mathrm{W\ m^{-2}\ sr^{-1}}$)/top of atmosphere irradiance (in $\mathrm{W\ m^{-2}}$) × cos(solar zenith angle). The second step is problematic as there is currently no atmospheric correction algorithm valid for highly turbid waters. The solution commonly adopted to estimate and remove the aerosol contribution from data recorded at the top of the atmosphere is the dark pixel method (Hu et al., 2000; Doxaran et al., 2002; Miller and McKee, 2004). The darkest pixel in the image is used to estimate the aerosol contribution throughout the entire scene. This approach assumes that the aerosol type and size distribution does not change significantly between the dark pixel and the study area. This assumption may not be valid and relies on the selection of the dark pixel target which is time-consuming and may be somewhat arbitrary.

The alternative and original solution proposed in this study is to use the 'surface reflectance' MODIS land product also available at full spatial resolution (MOD09GQ and MYD09GQ products for MODIS Terra and Aqua, respectively). Surface reflectance data are geolocated and correspond to the upwelling radiance above sea level obtained from the radiance signal recorded at the satellite level and corrected for atmospheric effects, multiplied by π and divided by the downwelling irradiance above sea level. MODIS L1B data, used as primary input, are corrected for the effect of gaseous absorption, molecules and aerosol scattering, coupling between atmospheric and surface bi-directional reflectance function and adjacency effect (Vermote et al., 1997). Gaseous absorption and molecular scattering are computed based on the viewing and solar angles and using look-up tables. The aerosol scattering is computed using dark targets (e.g. green forests) for which empirical relationships have been established between the visible and short wave infrared reflectance based on long-term data recorded by sun-photometers (Kaufman et al. 1997). The result is an estimate of the seawater reflectance which is not accurate enough for open ocean applications but a priori appropriate in the case of highly reflective estuarine waters. Note that the data are not corrected for skylight reflection at the air–water interface. However, Doxaran et al. (2004) showed that these effects are limited in turbid estuarine waters when considering a spectral ratio of above-water upwelling radiance between near-infrared and red wavelengths (see their Figs. 6 and 7). To test whether the use of surface reflectance data is suitable in our study, a direct comparison was made between the following MODIS Terra products: MOD02QKM (calibrated reflectance at the top of the atmosphere, noted Rtoa (Miller and McKee, 2004), then water reflectance estimated as $R\text{toa} - R\text{dp}$ where Rdp is the reflectance of the selected dark pixel recorded at the top of the atmosphere) and MOD09GQ (surface reflectance, noted R). As an illustration, the results obtained from data recorded over the Gironde estuary on 04/06/2005 are presented (Fig. 2). On this day, the darkest pixel was located less than 10 km westward and about 20 km southward from the mouth of the estuary. The reflectance signals recorded over this dark pixel, noted Rdp(B1) and Rdp(B2), were assumed to represent the atmospheric reflectances. Along a transect following the main navigation channel from the center to the mouth of the estuary (Fig. 1), the contribution of the water reflectance to the signal recorded at the top of the atmosphere was calculated as: $(R\text{toa} - R\text{dp})/R\text{toa}$, in %. Not surprisingly based on observations made by Doxaran et al. (2002), the turbid estuarine waters contribute to about 80% of the signal recorded at the top of the atmosphere in the red part of the spectrum (B1). This contribution is even higher in the near-infrared (B2), varying from 70 (near the mouth) to 90% (in the maximum turbidity zone). Therefore, on a clear day, the signal recorded over the estuary at the top of the atmosphere mainly results from the water contribution, so that the accuracy of atmospheric corrections is not crucial. This statement remains true when reflectance ratios are considered between the spectral bands B1 and B2. Along the same transect following the main navigation channel (data recorded on 04/06/2005), the ratios $[(R\text{toa} - R\text{dp})(\text{B2})/(R\text{toa} - R\text{dp})(\text{B1})]$ (here used as a reference), $[R\text{toa}(\text{B2})/R\text{toa}(\text{B1})]$ and $[R(\text{B2})/R(\text{B1})]$ are almost equal (see insert in Fig. 2). Note that these observations are only valid in the case of highly reflective waters; the atmospheric contribution grows rapidly as the water turbidity decreases, e.g. moving westward the mouth of the estuary, and reaches progressively up to 100% of the signal at the top of the atmosphere. But when considering the turbid Gironde estuarine waters, Eq. (2) can be directly applied to MODIS surface reflectance data, to a first approximation. For a practical and operational point of view, the surface reflectance product was therefore used in this study.

One year (01/01/2005 to 31/12/2005) of archived 'surface reflectance' MODIS data recorded over the Gironde estuary was downloaded from the NASA website: http://edcdaac.usgs.gov/modis/dataproducts.asp. Images where at least 90% of the Gironde estuary appeared under a cloud-free sky were selected for further processing. In 2005, a monthly minimum of five (February and April) and a maximum of 16 (May and June) cloud-free days were observed (Table 2). A resulting average of nine cloud-free days, thus potentially 16 MODIS (Terra plus Aqua) images, exploitable per month was obtained.

Land and cloud masks were applied to near-infrared B2 data by imposing the value of 0 to any surface reflectance greater than 25%. The surface reflectance ratio ($\Re_{21}$) was then calculated and Eq. (2) was applied to retrieve SPM concentrations. In the Gironde estuary, Irigoien and Castel (1997) observed a very good correlation between the diffuse downwelling attenuation coefficient (Kd, in m^{-1}) in the visible spectral region (400–700 nm) and SPM (in g m^{-3}): $\text{Kd} = 0.13 + 0.049 \times \text{SPM}$, $R^2 = 0.88$. Thus, the euphotic depth where light intensity falls to 1% of that at the surface (Zeu in meters, estimated as 4.6/Kd) decreases with increasing SPM concentration according to a power-law function. This results in Zeu values of 7, 1.8, 0.9 and 0.09 m, respectively, for SPM concentrations of 10, 50, 100 and 1000 g m^{-3}. The concentration maps produced from MODIS data are thus limited to surface waters (typically 0–1 m depth, depending on SPM concentration).

3. Results and discussion

3.1. Validation of the remote sensing algorithm

The first step was to determine how accurately SPM concentrations can be retrieved from MODIS satellite data. SPM concentrations measured in situ on the Marel platforms were simply compared to those retrieved from satellite data in the pixel containing the Marel platform. The sections of the estuary are narrow in Bordeaux, Portets and Libourne (respectively about 500, 200 and 200 m wide), so that strong land contamination affects MODIS full spatial resolution (250 m) data. Consequently, only the Pauillac Marel platform was considered, where the section of the estuary is 5000 m wide. As the platform is close to the shore, the first pixel right beside the platform and fully over the water was systematically selected on MODIS images.

A direct comparison between in situ measured and satellite derived concentrations required the following assumptions:

(1) The turbidity of surface waters was homogeneous over the satellite pixel beside the Marel platform and did not change significantly in time between the closest in situ and satellite measurements (maximum time difference of 5 min);
(2) The water turbidity was homogeneous within the first meter below the surface (as the turbidity sensor on the Marel platform is at a fixed depth of 1 m, while the optical depth viewed and analyzed by the satellite can be lower than 1 m);
(3) Adjacency effects (land contamination of satellite pixels over the water close to the shore) were limited on the $R(\text{B2})/R(\text{B1})$ spectral ratio.

A total of 116 MODIS Terra and 116 MODIS Aqua satellite images were processed in 2005. However, only images where the Pauillac Marel platform clearly appeared without any suspicious haze or remaining cloud contamination were considered for match-ups. As a result, 62 and 75 match-ups were finally identified in 2005 between field and, respectively, MODIS Terra and Aqua satellite data. Comparisons between field measured and satellite derived SPM concentrations (Fig. 3) globally showed a good agreement for both sensors for the entire SPM concentration range encountered (77–2182 g m^{-3}). Points are well distributed along the 1:1 relationship (Fig. 3). Linear regressions were fitted successively to the data and log-transformed data. Statistical analyses (Table 1) show that the intercept of the linear regressions is never significant and the slope is not significantly different from 1. The mean relative differences observed between field measured and satellite derived concentrations are 4.5 and −1.2%, respectively, for MODIS Terra and Aqua sensors. This indicates that satellite derived SPM concentrations were neither systematically underestimated nor overestimated. Considering SPM concentrations derived from Marel turbidity measurements as ground-truth, the mean absolute relative differences (regardless of the sign) observed with MODIS Terra and Aqua derived concentrations are, respectively, 22.27% (min. 0.4%, max. 82.4%) and 17.95% (min. 1.8%, max. 72.9%).

Given the assumptions made, the imperfect atmospheric corrections applied and also the potentially significant land contamination on first satellite pixels close to the shore, this result is quite satisfactory for the scope of this study. Results would certainly have been better if the Marel platform was located in the middle of the estuary (as far as possible from the shore).

3.2. Tidal dynamics of surface suspended particulate matter

The first objective was to compare the information obtained from field Marel and satellite MODIS data, in terms of tidal dynamics of surface SPM.

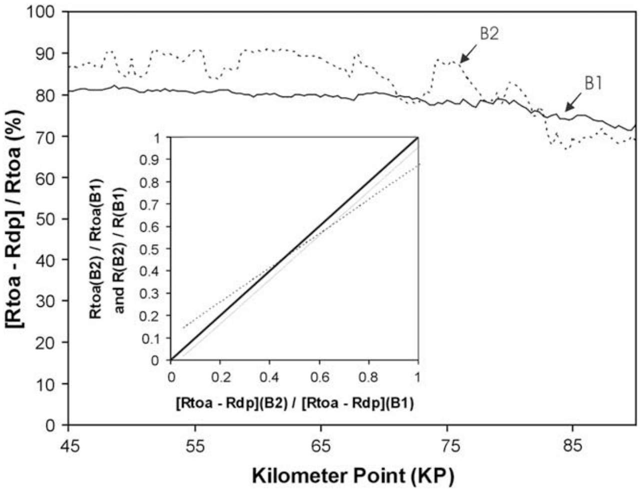

Fig. 2. Estimation of the water reflectance contribution to the reflectance signal recorded at the top of the atmosphere (*R*toa) along a transect following the main navigation channel of the estuary, from KP 90 (mouth) to KP 45. MODIS data (calibrated radiances) were recorded on 04/06/2005. The water contribution is calculated as the ratio (*R*toa − *R*dp)/*R*toa, expressed in %, where *R*dp is the top of the atmosphere reflectance of the darkest pixel in the coastal waters surrounding the estuary. The solid and dashed lines represent the B1 and B2 spectral bands, respectively. Insert: plot of the [*R*toa(B2)/*R*toa(B1)] (dashed line) and [*R*(B2)/*R*(B1)] (solid line) ratios as a function of [(*R*toa − *R*dp)(B2)/(*R*toa − *R*dp)(B1)], along the same transect. The thick line shows the 1:1 relationship.

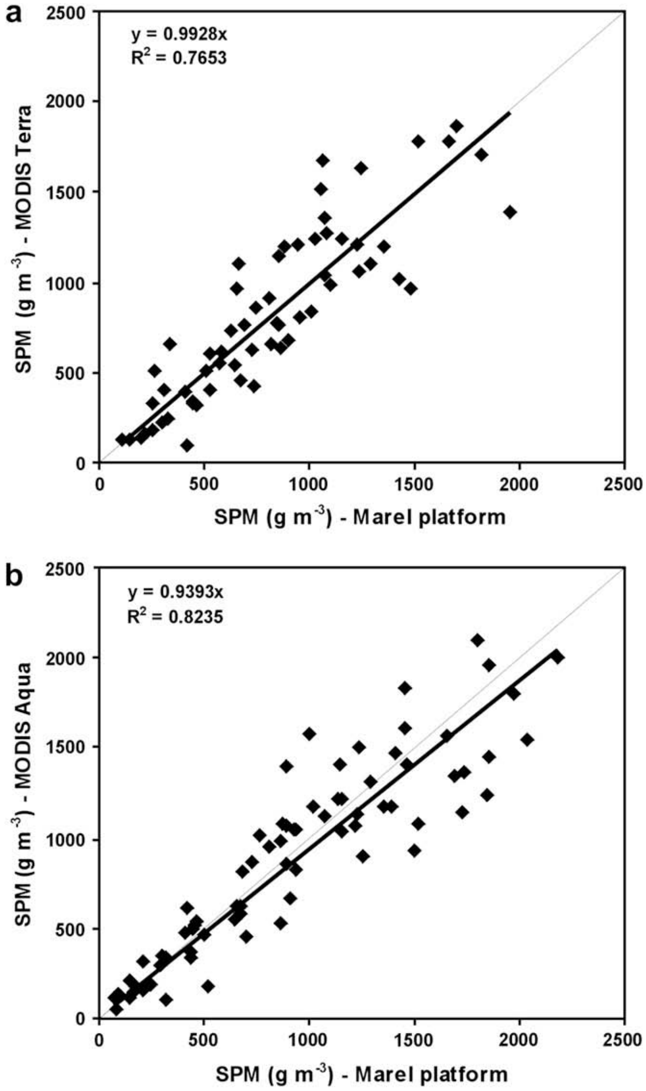

Fig. 3. Comparisons between surface SPM concentrations retrieved from satellite data and measured in situ on the Pauillac Marel platform. Linear plots for MODIS Terra (a) and MODIS Aqua (b); the thin and thick lines show, respectively, the 1:1 relationship and best linear regression with nil intercept.

Representative measurements recorded on Marel platforms show that surface water turbidity and salinity vary according to daily cycles of about 12.5 h (Fig. 4). At Pauillac (central estuary), turbidity is minimum at high water (maximum salinity) due to dilution by clear oceanic waters and settling of particles. Turbidity increases gradually during the ebb tide and peaks around low water (minimum salinity). Significant variations are then observed due to settling and resuspension phenomena. After low water, it decreases gradually during the flood tide. These variations systematically observed in Pauillac also apply but are less significant in the upstream platforms of the Garonne and Dordogne rivers. Fortnightly 15-day lunar cycles affect the amplitude of turbidity variations: it increases from mean to spring tides (e.g. Fig. 4a) and decreases from mean to neap tides (e.g. Fig. 4b). Similar SPM variations due to spring–neap tides have been measured by Mitchell et al. (2003) in the Trent estuary, over a 1-year period, using a continuous turbidity sensor.

Fig. 5 shows typical SPM concentration maps retrieved daily from MODIS Terra and Aqua data. High and low river flow periods (07/02/2005 during spring tide conditions and 22/06/2005 during mean tide conditions, respectively) are illustrated. High water time is indicated at Richard, which is located half-way between the mouth and confluence of the rivers (see Fig. 1). Note that high water occurs about 1 h earlier and 1 h after, respectively, at the river mouth and at Bordeaux. In both cases the retrieved SPM concentration ranges and gradients along the estuary are quite realistic and compare well with previous SPOT-HRV and Landsat-ETM+ satellite observations (Doxaran et al., 2002, 2006). Moreover, a good consistency is observed between the concentrations retrieved on the same day from the MODIS Terra and Aqua sensors; the SPM variations show the transport of water masses and SPM during the daily tidal cycle (see Fig. 5a,c as compared to b,d, respectively). On both dates, images were recorded about 3 h before high tide, i.e. around mid-flood. As expected, SPM maps derived chronologically from MODIS Terra then Aqua data (with a 1 h 40 min time difference) showed the upstream transport of SPM and decrease of water turbidity (through dilution by clear oceanic waters and settling of particles towards slack tide).

In order to study the influence of fortnightly tidal cycles, SPM maps retrieved from MODIS data were classified, each month, into three different categories based on tidal conditions at the time of satellite overpass in the Gironde area:

Table 1
Statistics concerning the linear regressions fitting the SPM concentrations derived from MODIS data and SPM concentrations measured on the Pauillac Marel station. The slope, intercept, determination coefficient (R^2), root-mean-square (rms) and standard deviation (SD) are presented for each regression, including for log-transformed data.

Linear regression	Slope	Intercept	R^2	rms	SD
Terra/Marel	0.9474	47.844	0.7676	228.11	230.00
Terra/Marel	0.9928	0	0.7653	229.22	230.87
Aqua/Marel	0.8681	89.282	0.8312	238.36	240.02
Aqua/Marel	0.9393	0	0.8235	244.97	245.78
Log-transformed Terra/Marel	1.0266	0.093	0.7987	0.14	0.14
Log-transformed Terra/Marel	0.9943	0	0.7979	0.14	0.14
Log-transformed Aqua/Marel	0.9586	1.100	0.8822	0.13	0.13
Log-transformed Aqua/Marel	0.9932	0	0.881	0.13	0.13

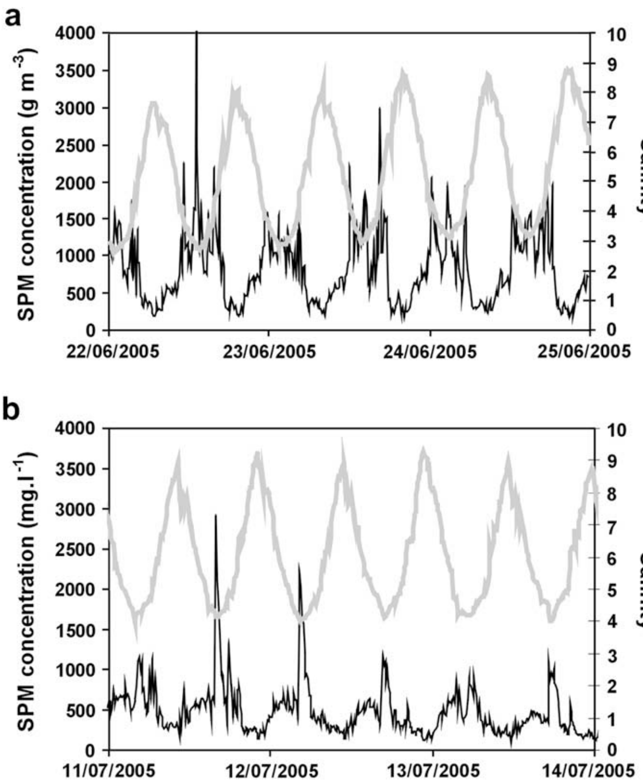

Fig. 4. Typical measurements 1 m below the water surface (turbidity converted into SPM concentration (black line) and salinity (grey line)) recorded on the Pauillac Marel platform in June 2005 with increasing tidal range (i.e. from mean to spring tides) (a); in July 2005 with decreasing tidal range (i.e. from mean to neap tides) (b).

(1) Neap tides, when MODIS data acquisition systematically occurs around high tide;
(2) Mean tides, when MODIS data acquisition occurs at any other moment of the tide;
(3) Spring tides, when MODIS data acquisition systematically occurs around low tide.

The SPM maps retrieved in January 2005 (Fig. 6) are representative of the results obtained the other months of the year. The neap-tide map shows the upstream location of the TM and minimum surface SPM concentrations in the estuary (Fig. 6a), as could be expected from field data (e.g. see Fig. 4b). On the contrary, the spring-tide map shows the extreme downstream location of the TM and maximum surface SPM concentrations (Fig. 6c), again in agreement with field observations (e.g. see Fig. 4a). The dynamics of surface SPM along the fortnightly tidal cycle can be clearly observed using satellite data (Fig. 6a,bc). These variations of SPM concentrations highlight the predominant influence of tidal currents on the resuspension of bottom sediments and mixing within the water column. Each month in 2005, surface SPM concentrations typically increased by a factor of 10–50 between the two extreme tidal conditions, i.e. between neap tides/high water conditions and spring tides/low water conditions. As a result, during spring tides, the TM can be easily located using satellite observations limited to surface waters. Note that satellite data systematically show strong SPM concentration variations along a section of the estuary (i.e. from the left to the right shore). These variations can be related to the bathymetry and current velocities. Observations made on Marel platforms at fixed geographical locations are therefore not necessarily representative of the mean water turbidity within a transversal section of estuary.

3.3. Seasonal dynamics of the turbidity maximum zone

Field and satellite data available in 2005 were analyzed to describe the seasonal dynamics of the TM in the estuary. Our intent was to identify the periods (and environmental conditions) when the TM grew from river inputs, and when it was partially expelled towards the ocean, and finally to estimate the masses of sediments involved.

3.3.1. Field observations (upstream part)

The SPM concentrations obtained from turbidity measurements onboard the four Marel platforms were averaged monthly then related to relevant freshwater discharge records (Dordogne for Libourne, Garonne for Portets, Garonne for Bordeaux and Gironde (i.e. Dordogne + Garonne) for Pauillac) (Fig. 7). In winter when freshwater inputs were at a maximum (January to April and December), SPM concentrations were at a minimum in the rivers (Fig. 7a,b) and maximum in Pauillac (Fig. 7d). The TM was therefore pushed downstream by the high river flow. In June, the river flow significantly decreased and the TM moved into the rivers, where SPM concentrations became extremely high (Fig. 7a,bc). The situation remained almost unchanged over 4 months (July to October). Then the river flow increased and the TM was again pushed downstream. The TM appeared to be diluted in Pauillac during the winter, hence probably extended to the central and downstream parts. River floods are known to supply consecutively highly turbid waters then clear freshwater in the central and lower estuary, which results in both fluid mud formation and a dilution process within the water column. Over the year, the proportion of freshwater in the estuary typically increases from 30 to 60% between the low river flow and high river flow periods (Castaing, 1981). Note that similar runoff-induced movements of the TM have been documented in other macrotidal estuaries (e.g. Uncles et al., 2006)

3.3.2. Satellite observations (central and lower estuary)

The seasonal movements of the TM can be observed by comparing the month-to-month TM location during spring tides (Fig. 8). In January, the TM was spread over 40 km. A main TM was located in the central estuary while a second TM was also formed in the lower part. In March and May, the location of the two TM remained unchanged but SPM concentrations significantly decreased in the central and lower estuary while they increased in the Garonne and Dordogne rivers. This certainly resulted from significant export of SPM towards the ocean then upstream movement of the TM. SPM concentrations were heterogeneous and patchy, as already observed during the same period of the year using Landsat-ETM+ satellite data (Doxaran et al., 2006). High SPM concentrations could be observed near the large intertidal mudflats in the mouth area, which suggests intensive sedimentation and resuspension processes.

During the summer period (Fig. 8), the TM moved upstream, notably in the rivers, as already observed from Marel data (Fig. 7). In October, as the river flow increased, the TM location remained almost unchanged but SPM concentrations significantly increased. Finally in December, as the river flow reached a maximum, SPM concentrations increased in the upper and central estuary due to river input (as indicated by field Marel data, see Fig. 7). Also, a part of the TM detached from the main TM and moved in the lower estuary, as already observed in January. The existence of the first TM throughout the year is certainly due to the morphology of the estuary: a narrow central part with islands and high bottoms, where the fluid mud from the main channel is regularly rejected (dredging activities). The maximum SPM concentrations were found in this first TM. The presence of the second TM is related to the hydrodynamic conditions (Sottolichio et al., 2001). In another macrotidal environment (the Scheldt), Chen et al. (2005) identified

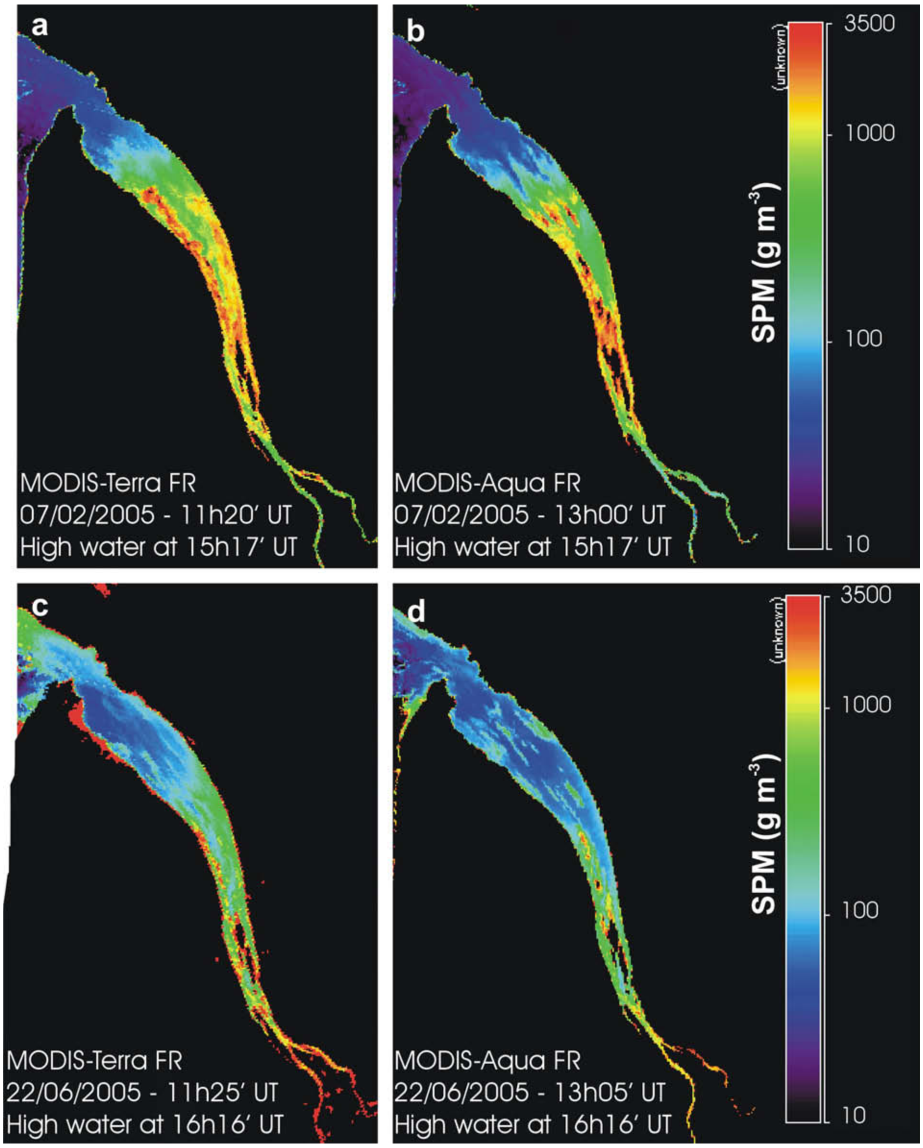

Fig. 5. Examples of surface SPM concentration maps established in the Gironde estuary using MODIS Terra and Aqua full resolution data: the 07/02/2005 during a high river flow period and spring tide conditions (a and b, respectively); the 22/06/2005 during a low river flow period and mean tide conditions (c and d, respectively). High water is indicated at Richard (KP 72).

three TM the existence of which was related to the energy distribution pattern in the estuary: (1) a marine-dominated TM near the mouth mainly controlled by the tidal energy; (2) a river-dominated TM in the upper estuary which depends on river supply; and (3) a tide-dominated TM (the most important) in the middle estuary which coincides with the total energy maximum. To a certain extent, the situation is similar in the Gironde but with higher SPM concentrations and a significantly stronger influence of the river discharge (which is more than twice that of the Scheldt) over the whole estuary and a permanent trapping of SPM occurring in the central part due to the morphology of the estuary.

Throughout the year, SPM concentrations in surface water in the estuary were observed to vary by a factor of 1–5, which remains low compared to variations induced by fortnightly tidal cycles. Therefore, tidal cycles predominantly controlled the SPM concentrations while the river flow mainly controlled the location of the TM and its seasonal movements along the estuary.

Annual variations of the monthly-averaged SPM concentrations retrieved from satellite data in the pixel containing the Pauillac Marel platform were close to the ones measured on the platform (see Fig. 7d). This proves that the influence of tidal cycles can be removed from satellite observations to obtain information on monthly movements of the TM. This requires a sufficient number of cloud-free satellite images recorded each month during the different periods of the fortnightly tidal cycle, i.e. during neap, mean and spring tide conditions. This was the case in 2005 (see Table 2).

3.4. Seaward export and mass balance of the turbidity maximum zone

The information available from field (Marel) and satellite (MODIS) data was finally used to (1) determine conditions in which the seaward export of SPM occurred; and (2) to estimate the SPM mass balance in the estuary during the year 2005Table 3.

On average, the total mass of suspended sediments (including fluid mud) in the estuary is estimated to vary between about 4 and 6×10^6 tons from a wet to a dry year (Castaing, 1981). The SPM river

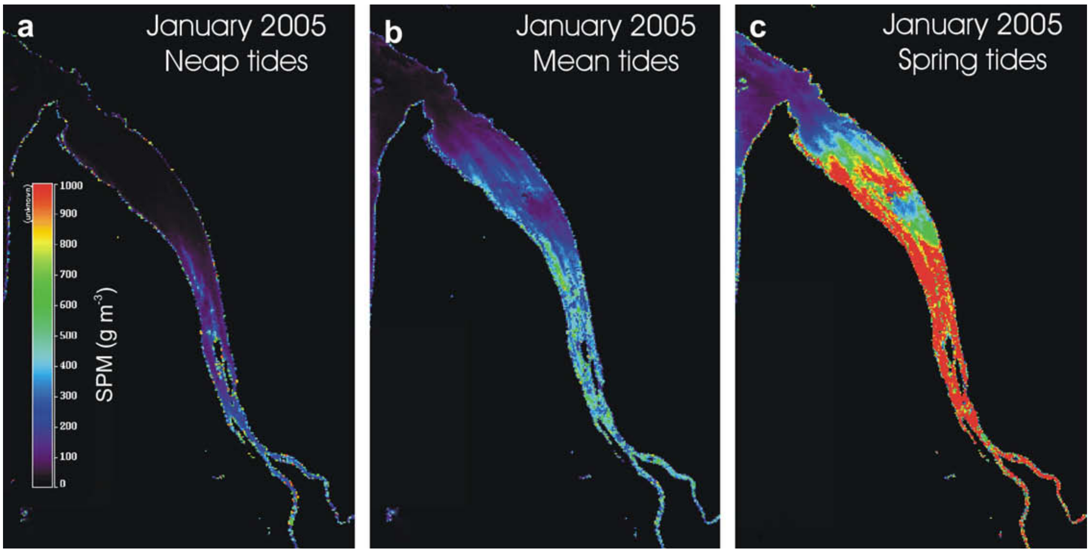

Fig. 6. Variations of surface SPM concentrations in the Gironde estuary observed in January 2005 using MODIS Terra and Aqua full resolution data during neap, mean and spring tides (a, b and c, respectively).

input is about of 3.2×10^6 tons on a wet year (Schäfer et al., 2002) and about 2×10^6 tons on a dry year (Castaing, 1981). As a consequence, in order to maintain the same mass of sediments in the estuary over 1 year, about half the TM ($\sim 2.5 \times 10^6$ tons of sediments) is expected to be expelled either towards the ocean or to sediment. In the Gironde estuary, Allen et al. (1980) observed a mean yearly sedimentation rate of silt and clay of 1.6×10^6 tons between 1900 and 1973. This would represent a flux of about 1×10^6 tons of SPM expelled on average every year to the ocean. We analyzed the variations of SPM concentrations in the mouth area, used as an indicator of probability of SPM export into the ocean. These variations were related to several environmental factors expected to control this seaward export.

3.4.1. *Seaward export and controlling factors*

The monthly-averaged SPM concentration in the whole mouth area (KP 90–KP 95), observed during spring tides and around low tide, was compared successively to the monthly-averaged:

(1) Gironde freshwater discharge (Fig. 9a);
(2) Tidal range (Fig. 9b);
(3) Mean SPM concentration in the [KP 75–KP 80] section, used as an indicator of fluid mud deposits in the lower estuary (Castaing and Allen, 1981) (Fig. 9c);
(4) Wind speed and direction at the mouth of the estuary (Fig. 9d). Wind data obtained from QuikScat satellite data were downloaded from the Remote Sensing Systems web site http://www.remss.com/qscat/).

The surface SPM concentration in the mouth area was high in January, which indicates that a part of the TM was potentially expelled towards the ocean. The concentration was low in February and again high during the March equinox. It was again low in April before reaching its annual peak in May during spring floods. It then decreased gradually down to its minimum value reached in August, increased again in September and October, then reached a plateau and even slightly decreased in November and December.

The river discharge apparently controlled the SPM concentration in the mouth area at least from May to October (Fig. 9a). The influence of the tidal range was much more limited except during the equinoxes of March and September; the increase of the tidal range systematically resulted in higher SPM concentrations (Fig. 9b). The presence of fluid mud in the lower estuary appeared as the main factor controlling water turbidity from January to July (Fig. 9c). Throughout the year, the wind was blowing from the north (except in October) and apparently did not much influence water turbidity in the mouth area (Fig. 9d). During the winter and early spring periods, the high river discharge, presence of fluid mud in the lower estuary and decreasing wind speed combined to favor the export of SPM towards the ocean. The conditions were optimal in May (maximum river flow, presence of fluid mud and resuspension processes which occurred during the March equinox) for a massive seaward export.

3.4.2. *Use of surface concentration as a marker of sediment total mass*

Lastly, the mean surface SPM concentration in the estuary excluding the rivers (KP 25–90) was calculated each month from MODIS satellite data. The tidal influence can be significantly filtered out on monthly-averaged SPM concentrations retrieved from MODIS data (see Fig. 7d). Therefore, we used the monthly variations of the mean surface SPM concentration in the estuary to estimate the variations of the total mass of SPM in the estuary. We considered that variations of the SPM total mass could only result from: (1) export towards the ocean; (2) supply from (or move to) the rivers upstream KP 25; and (3) sedimentation in the estuary including the mudflats along the shores.

Variations of the mean SPM concentration in the estuary in 2005 are presented in Fig. 10. The mean SPM concentration in January (522 g m^{-3}), taken here as a reference, decreased in February (−15%), then March (−38%) and April (−46%) when it reached its minimum value (279 g m^{-3}). According to field (Marel) data (Fig. 7), most of the TM was located downstream from Bordeaux during this period. Consequently it may be concluded that between January and April about half (46%) the TM was either expelled towards the ocean or settled as sediments. This estimate is realistic but probably inaccurate as a decrease in the river flow in March has apparently resulted in SPM migration inside the rivers at least as far as Bordeaux (Fig. 7c). In May, due to peak river floods, the SPM concentration in the estuary strongly increased and peaked at 673 g m^{-3}. This most likely resulted from river inputs and resuspension from mudflats in the mouth area (see Fig. 8). Just after peak floods, the

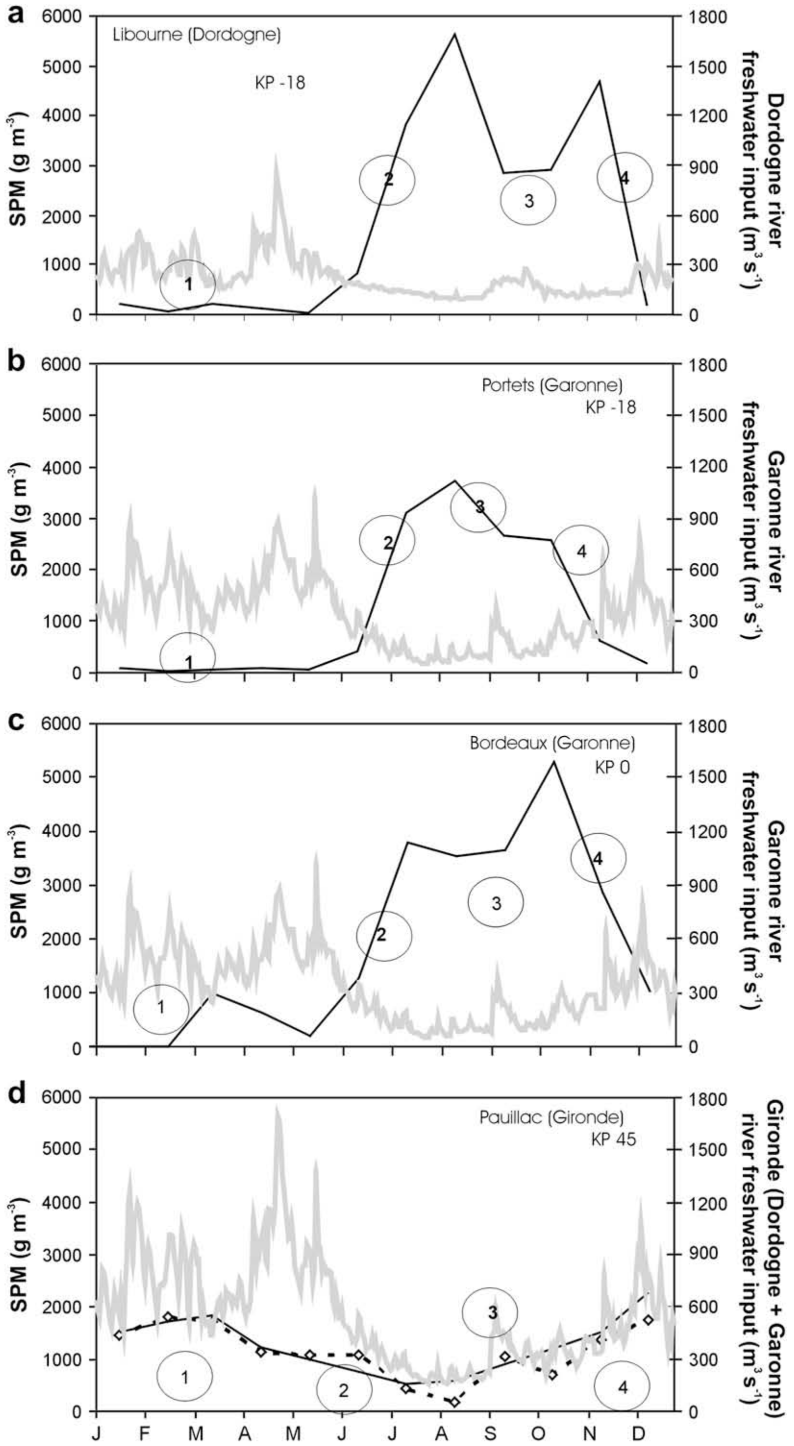

Fig. 7. Monthly-averaged surface SPM concentration measured on the Marel platforms of Libourne (a), Portets (b), Bordeaux (c) and Pauillac (d) in 2005. The daily freshwater discharges of, respectively, the Dordogne, Garonne and Gironde (Garonne + Dordogne) rivers are overplotted. The monthly-averaged SPM concentration retrieved from MODIS data in Pauillac (white points) is compared to the one measured on the Marel platform (d). Four specific TM situations are highlighted: the winter period when the TM is diluted and located in the lower estuary (1); the quick upstream move occurring in June (2); the summer period when the TM is concentrated inside the rivers (3) and the quick downstream move in November and December (4).

SPM concentration gradually decreased down to a minimum value of 279 g m−3 in August, as it did in April. This occurred as the main TM moved upstream inside the rivers (Fig. 7a,b,c and Fig. 8). From September to December, the mean SPM concentration in the estuary increased gradually due to river inputs and to downstream migration of the TM from the rivers (Figs. 7 and 8). In December, the mean SPM concentration had risen to the value initially observed in January (543 g m−3 as compared to 522 g m−3). It may be concluded that about half the TM total mass (about 3×10^6 tons of SPM) was either expelled towards the ocean or settled to the bottom as sediments during the winter and spring periods. Then during spring peak floods, autumn and winter, river inputs and resuspension processes over mudflats had re-filled the estuary almost up to its initial mass. In macrotidal

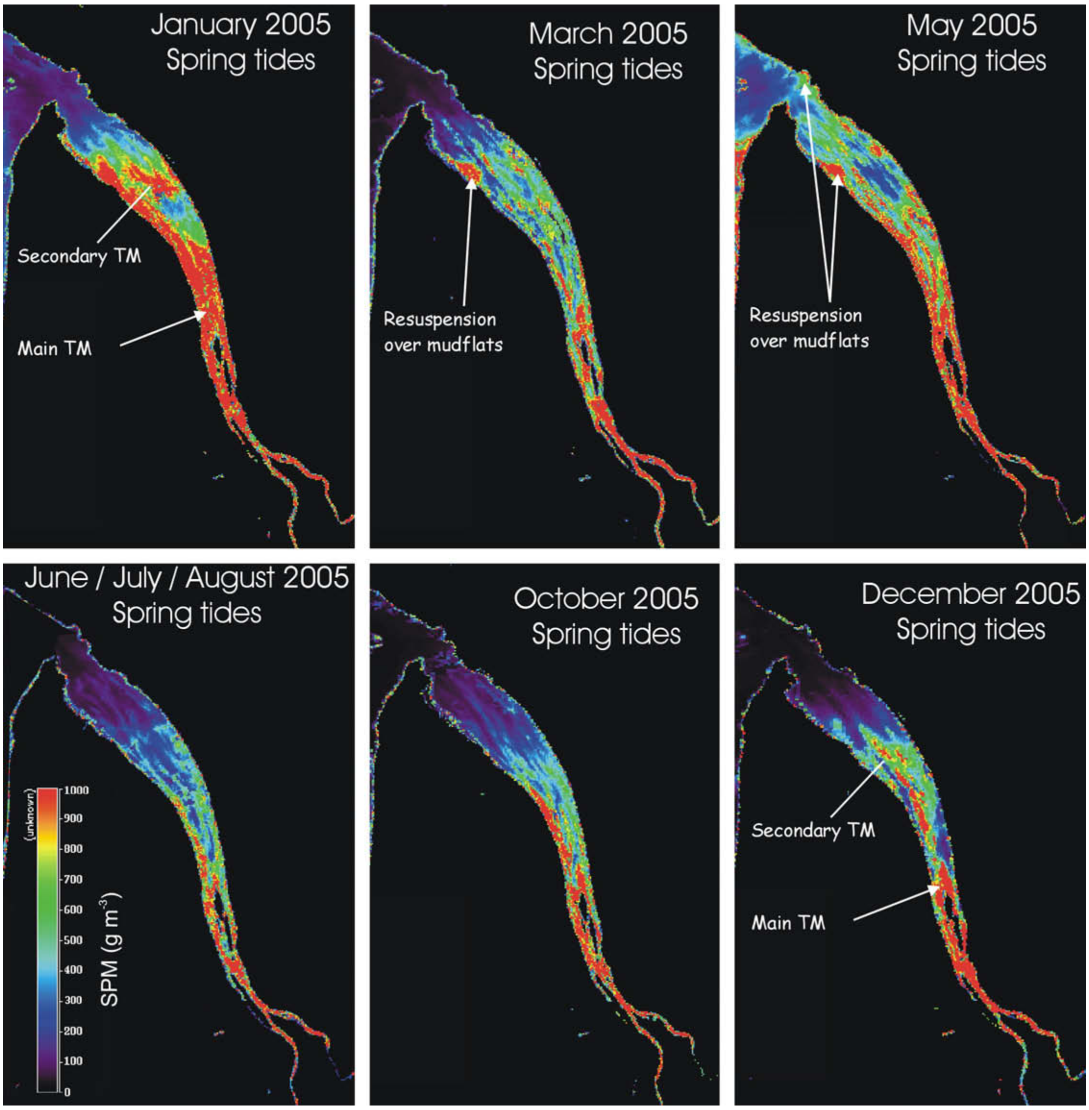

Fig. 8. Seasonal variations of surface SPM concentrations retrieved from MODIS Terra and MODIS Aqua satellite data of the Gironde estuary. SPM maps were produced from MODIS data recorded over the estuary during spring tide conditions and around low water at Richard.

estuaries such as the Seine (France), intertidal mudflats are known to play a key role in reducing the seaward export of sediments. In the Gironde, it is realistic to assume that the total mass of SPM in the estuary remained almost unchanged over the particularly dry year of 2005. To confirm these results, field measurements would be required to document typical SPM vertical profiles in the estuary (Doxaran, 2002) but also to locate and estimate the mass of fluid mud deposits in the TM (Le Hir et al., 2001a, b) and intertidal mudflats (Deloffre et al., 2006).

Table 2
Number of cloud-free MODIS Terra and MODIS Aqua images processed in 2005 to produce maps SPM concentrations in the Gironde estuary.

Month (2005)	MODIS Terra	MODIS Aqua	Month (2005)	MODIS Terra	MODIS Aqua
January	6	6	July	12	12
February	5	5	August	8	8
March	11	11	September	11	11
April	5	5	October	8	8
May	16	15	November	9	9
June	16	16	December	9	10

4. Conclusion

The dynamics of the TM in macrotidal estuaries plays an important role in the transfer of particulate material from the

Table 3
List of acronyms and notation.

B1	MODIS spectral band 1 (620–670 nm)
B2	MODIS spectral band 2 (841–876 nm)
ETM+	Enhanced Thematic Mapper Plus
HRV	High Resolution Visible
IFREMER	Institut Français de Recherche pour l'Exploitation de la MER
KP	Kilometer point, i.e. distance from Bordeaux in km
MODIS	Moderate Resolution Imaging Spectroradiometer
NASA	National Aeronautics and Space Administration
NTU	Nephelometric turbidity units
R	Seawater or surface reflectance (dimensionless)
$Rtoa$	Reflectance at the top of the atmosphere (dimensionless)
Rdp	Reflectance at the dark pixel (dimensionless)
$\Re$	Spectral band ratio of seawater reflectance
SPM	Suspended particulate matter
TM	Turbidity maximum zone

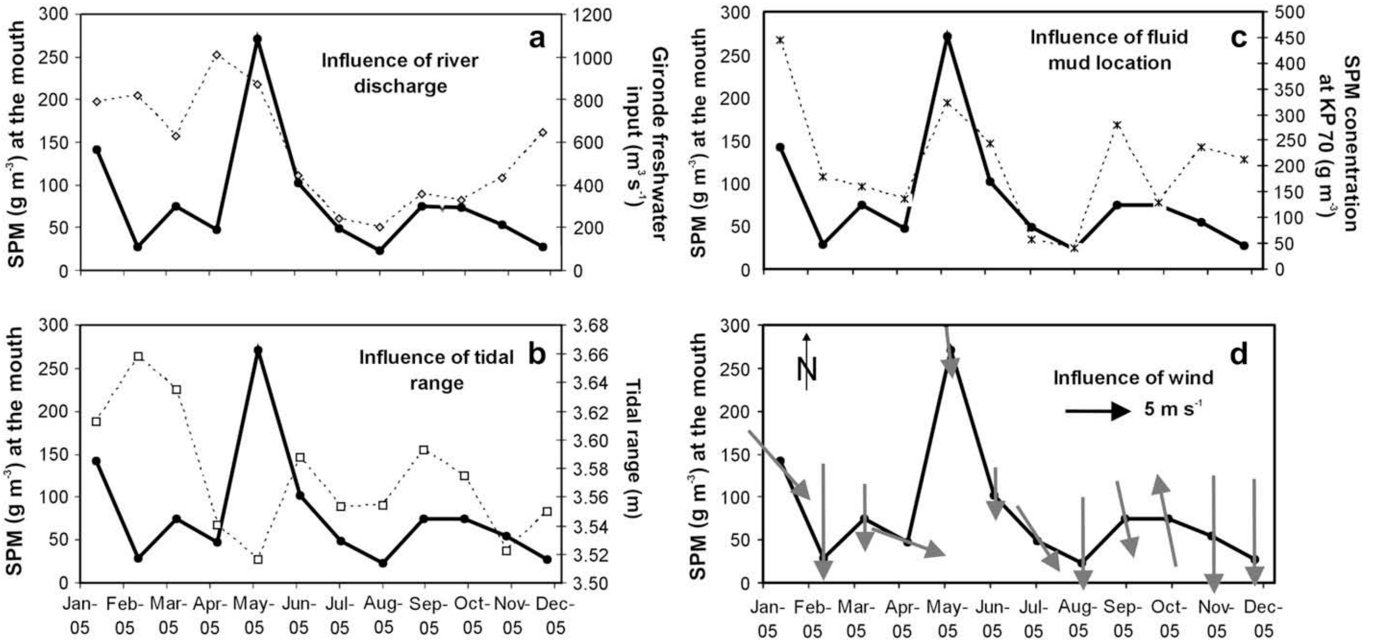

Fig. 9. Monthly-averaged surface SPM concentration observed from MODIS Terra and MODIS Aqua satellite data in the mouth section ($90 < KP < 95$) of the Gironde estuary, during spring tides and around low tide. Overplot of the monthly-averaged Gironde freshwater input (a), tidal range, (b) SPM concentration in the downstream part ($65 < KP < 75$) of the estuary, which indicates the presence of fluid mud (c) and wind regime in the mouth area (speed and direction compared to the north).

continent to the ocean. These dynamics are complex and require new methodologies to estimate sedimentary fluxes exported to the ocean. The present study proved that such information can be obtained through combining complementary field (measurements onboard fixed platforms) and satellite ocean color data. Field data potentially provide almost continuous measurements to study daily tidal cycles and allow sampling confined to parts of the estuary that cannot be analyzed using remote sensing. They also provide match-ups to validate satellite observations. Combined satellite and field data give an overview of the tidal and seasonal dynamics of suspended sediments in the whole estuary. MODIS satellite data, and the so-called 'surface reflectance' product, were proved to be operational to quantify SPM concentrations in turbid sediment-dominated surface waters. In the Gironde estuary, SPM concentrations were retrieved with uncertainties of 22 and 18% from MODIS Aqua and MODIS Terra data, respectively, when applying the algorithm developed by Doxaran et al. (2002). These uncertainties were obtained based on 62 and 75 match-ups identified in 2005.

Based on these new observations, the seasonal dynamics of the TM proved to be more complex than suggested by earlier studies (e.g. Castaing and Allen, 1981; Sottolichio et al., 2001). Several TM were identified: (1) a first TM, almost permanent, the existence of which is related to the morphology of the estuary; (2) a second TM, called dynamic TM, the location and movements of which are mainly controlled by the river discharge (while the tidal range controls its horizontal extent); and (3) several minor TMs around resuspension areas such as intertidal mudflats. These observations are rather concordant with results obtained by Chen et al. (2005) who also identified several TM co-existing in the Scheldt estuary. In the Gironde in 2005 (dry year), these TM followed an annual cycle with seasonal movements. The export of sediments to the ocean occurred when several conditions were combined: presence of fluid mud in the lower estuary, peak flood, resuspension due to high tidal range and limited wind. The mean surface SPM concentration in the whole estuary (excluding the rivers) also varied according to an annual cycle, closely related to the movements of the TM, and remained almost unchanged on a 1-year

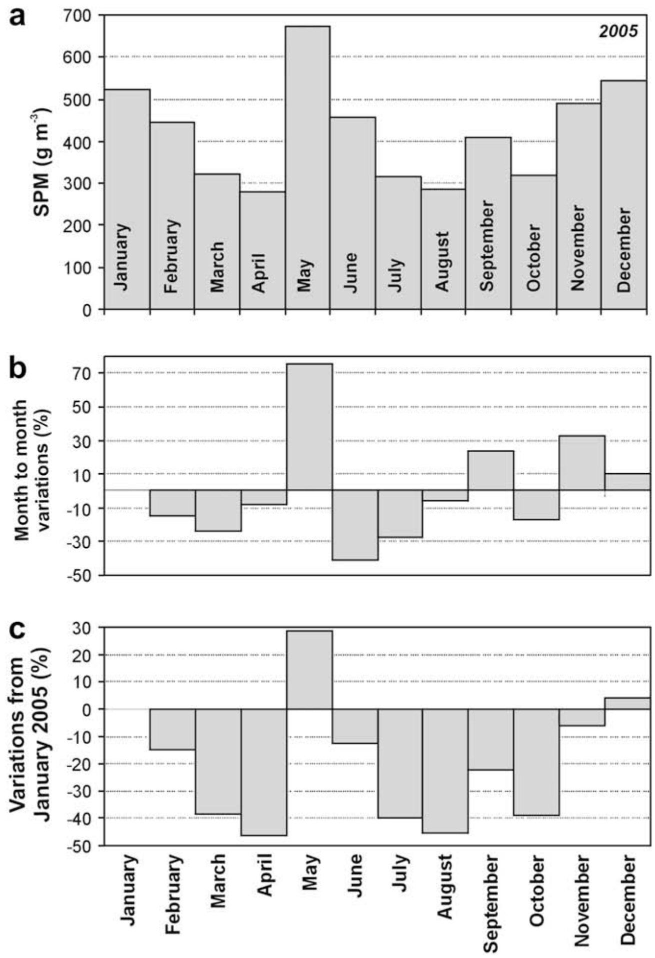

Fig. 10. Monthly-averaged surface SPM concentration in the Gironde estuary ($25 < KP < 90$, i.e. from the confluence of the rivers to the mouth) observed in 2005 from MODIS satellite data (a). Month to month concentration variation (in %) (b). Relative difference (in %) with the concentration in January 2005 (c).

basis. This probably indicates the conservation of the TM total mass in 2005. This suggests that river inputs have compensated for seaward export and sedimentation.

Surface SPM concentrations were mainly controlled by tidal cycles and varied by a factor of 10–50 between the two extreme tidal conditions. Seasonal variations of SPM concentrations were mainly controlled by the river discharge and were much more limited (factor of 1–5). On a seasonal basis, the role played by intertidal mudflats near the mouth in the temporary trapping of sediments inside the estuary, thus preventing the seaward export of SPM, remains unclear.

In the near future, additional field measurements should document the seasonal sedimentation rates on the intertidal mudflats, e.g. using field altimeter data (Deloffre et al., 2006). Ideally, field data should also provide: (1) information concerning the vertical profiles of turbidity in order to complement satellite observations limited to surface waters; and (2) bottom concentrations to detect the presence of fluid mud. A fifth Marel platform to be installed in 2010 near the mouth of the estuary (Fig. 1), equipped with sensors 1 m below the surface and 1 m above the seabed, will help in this domain. Then the next step will be to integrate field and satellite observations into a three-dimensional hydrodynamic and sediment transport model (e.g. Siegel et al., 1999; Sottolichio et al., 2001; Vos et al., 2000; Douillet et al., 2001). The development and operational use of an integrated data-modeling approach for SPM transport is a challenge in order to determine the fate of terrestrial particulate substances (SPM, nutrients, carbon) in coastal waters influenced by river inputs at regional and global scales (Schlunz and Schneider, 2000).

Acknowledgements

The authors want to thank the DAAC (NASA) and USGS for providing MODIS satellite data. The research was supported by a Marie Curie European Reintegration Grant (contract ERG-14905) and the Centre National d'Etudes Spatiales (CNES) in France. We are grateful to one anonymous reviewer for helpful comments.

References

Allen, G.P., Salomon, J.C., Bassoulet, P., Du Penhoat, Y., De Grandpré, C., 1980. Effects of tides on mixing and suspended sediment transport in macrotidal estuaries. Sedimentary Geology 26, 69–90.

Castaing, P., 1981. Le transfert à l'océan des suspensions estuariennes. Le cas de La Gironde. PhD thesis, University Bordeaux 1, France, 540 pp.

Castaing, P., Allen, G.P., 1981. Mechanisms of seaward escape of suspended sediment from the Gironde: a macrotidal estuary in France. Marine Geology 40, 101–118.

Chen, M.S., Wartel, S., Van Eck, B., Van Maldegem, D., 2005. Suspended matter in the Scheldt estuary. Hydrobiologia 540, 79–104.

Deloffre, J., Lafite, R., Lesueur, P., Verney, R., Lesourd, S., Cuvilliez, A., Taylor, J., 2006. Controlling factors of rhythmic sedimentation processes on an intertidal estuarine mudflat. Role of the turbidity maximum in the macrotidal Seine estuary, France. Marine Geology 255, 151–164.

Douillet, P., Ouillon, S., Cordier, E., 2001. A numerical model for fine suspended sediment transport in the south-west lagoon of New-Caledonia. Coral Reefs 20, 361–372.

Doxaran, D., 2002. Télédétection et modélisation numérique des flux sédimentaires dans l'estuaire de la Gironde. PhD thesis, University Bordeaux 1, France, 326 pp.

Doxaran, D., Froidefond, J.M., Lavender, S.J., Castaing, P., 2002. Spectral signature of highly turbid waters. Application with SPOT data to quantify suspended particulate matter concentrations. Remote Sensing of Environment 81, 149–161.

Doxaran, D., Froidefond, J.M., Castaing, P., 2003. Remote sensing reflectance of turbid sediment-dominated waters. Reduction of sediment type variations and changing illumination conditions effects using reflectance ratios. Applied Optics 42, 2623–2634.

Doxaran, D., Cherukuru, R.C.N., Lavender, S.J., 2004. Surface reflection effects on upwelling radiance field measurements in turbid waters. Journal of Optics A: Pure and Applied Optics 6, 690–697.

Doxaran, D., Castaing, P., Lavender, S.J., 2006. Monitoring the maximum turbidity zone and detecting fine-scale turbidity features in the Gironde estuary using high spatial resolution satellite sensor (SPOT HRV, Landsat ETM+) data. International Journal of Remote Sensing 27, 2303–2321.

Dyer, K.R., 1986. Coastal and Estuarine Sediment Dynamics. John Wiley and Sons, Chichester, 342 pp.

Fettweis, M., Sas, M., Monbaliu, J., 1998. Seasonal, neap–spring and tidal variation of cohesive sediment concentration in the Scheldt estuary, Belgium. Estuarine. Coastal and Shelf Science 47, 21–36.

Hedges, J.I., Keil, R.G., Benner, R., 1997. What happens to terrestrial organic matter in the ocean? Organic Geochemistry 27, 195–212.

Hu, C., Carder, K.L., Muller-Karger, F.E., 2000. Atmospheric correction of SeaWiFS imagery of turbid coastal waters: a practical method. Remote Sensing of Environment 74, 195–206.

Irigoien, X., Castel, J., 1997. Light limitation and distribution of chlorophyll pigments in a highly turbid estuary: the Gironde (SW France). Estuarine. Coastal and Shelf Science 44, 507–517.

Kaufman, Y.J., Tanré, D., Remer, L.A., Vermote, E.F., Chu, A., Holben, B.N., 1997. Operational remote sensing of tropospheric aerosol over land from EOS moderate resolution imaging spectroradiometer. Journal of Geophysical Research 102, 17051–17067.

Le Hir, P., Bassoullet, P., Jestin, H., 2001a. Application of the continuous modeling concept to simulate high-concentration suspended sediment in a macrotidal estuary. In: McAnally, W.H., Mehta, A.J. (Eds.), Coastal and Estuarine Fine Sediment Processes. Elsevier, Amsterdam, pp. 229–247.

Le Hir, P., Ficht, A., Silva Jacinto, R., Lesueur, P., Dupont, J.-P., Lafite, R., Brenon, I., Thouvenin, B., Cugier, P., 2001b. Fine sediment transport and accumulations at the mouth of the Seine estuary (France). Estuaries 24, 950–963.

Ludwig, W., Probst, J.L., Kempe, S., 1996. Predicting the oceanic input of organic carbon by continental erosion. Global Geochemical Cycles 10, 23–41.

Miller, R.L., McKee, B.A., 2004. Using MODIS Terra 250 m imagery to map concentrations of total suspended matter in coastal waters. Remote Sensing of Environment 93, 259–266.

Mitchell, S.B., Lawler, D.M., West, J.R., Couperthwaite, J.S., 2003. Use of continuous turbidity sensor in the prediction of fine sediment transport in the turbidity maximum of the Trent estuary, UK. Estuarine. Coastal and Shelf Science 58, 643–650.

Schäfer, J., Blanc, G., Lapaquellerie, Y., Maillet, N., Maneux, E., Etcheber, H., 2002. Ten-year-observation of the Gironde fluvial system: fluxes of suspended matter, particulate organic carbon and cadmium. Marine Chemistry 79, 229–242.

Schlunz, B., Schneider, R.R., 2000. Transport of terrestrial organic carbon to the oceans by rivers: re-estimating flux and burial rates. International Journal of earth Sciences 88, 599–606.

Siegel, H., Gerth, M., Mutzke, A., 1999. Dynamics of the Oder river plume in the Southern Baltic Sea: satellite data and numerical modelling. Continental Shelf Research 19, 1143–1159.

Sottolichio, A., Le Hir, P., Castaing, P., 2001. Modeling mechanisms for the turbidity maximum stability in the Gironde estuary. In: McAnally, W.H., Mehta, A.J. (Eds.), Coastal and Estuarine Fine Sediment Processes. Elsevier, Amsterdam, pp. 373–386. France.

Uncles, R.J., Stephens, J.A., Harris, C., 2006. Runoff and tidal influences on the estuarine turbidity maximum of a highly turbid system: the upper Humber and Ouse Estuary, UK. Marine Geology 235, 213–228.

Vermote, E.F., El Saleoql, N., Justice, C.O., Kaufman, Y.J., Privette, J.L., Remer, L., Roger, J.C., Tanré, D., 1997. Atmospheric correction of visible to middle-infrared EOS-MODIS data over land surfaces: background, operational algorithm and validation. Journal of Geophysical Research 102, 17131–17141.

Vos, R.J., Brummelhuis, P.J.G., Gerritsen, H., 2000. Integrated data-modelling approach for suspended sediment transport in a regional scale. Coastal Engineering 41, 177–200.